Journal of Marine Research, 43, 465–491, 1985

Seasonal oxygen cycling and primary production in the Sargasso Sea

by W. J. Jenkins[1] and J. C. Goldman[2]

ABSTRACT

The hydrographic record at Station S in the Sargasso Sea shows the development of a subsurface oxygen maximum within the euphotic zone which must be of photosynthetic origin. Consideration of insolation, heat budgets and available $^3He/^3H$ data yields an estimate of the order of 5 M m^{-2} y^{-1} for the vertically integrated oxygen production rate. Gas exchange calculations reveal a similar oxygen flux leaving the surface, and examination of respiration cycles below the euphotic zone yields consistent results. Such results point to new production of the order of 50 g C m^{-2} y^{-1}. By using a more realistic mixed layer-thermocline model (Klein and Coste, 1984) it appears that the flux of nutrients into the euphotic zone is sufficient to support such a production. The pulse-like nature of nutrient injection implied by this model raises the possibility of a spatially variable efficiency of recycling which may account for the disparity between the above observations and the level of new production inferred from ^{14}C and ^{15}N incubation techniques.

1. Introduction

One of the most important and fundamental questions facing marine biology today is the magnitude of "new" primary production in oligotrophic waters (Eppley, 1981). By "new primary production" we mean (as do Dugdale and Goering, 1967, and Eppley and Peterson, 1979) the amount of photosynthetically fixed carbon within and subsequently removed from the euphotic zone on timescales of the order of months. This question has bearing on the rate of biological activity and cycling of nutrients within the sea, the vertical fluxes and flux divergences due to oxidation of particles below the euphotic zone, and the vertical transport of many organic and inert substances linked to these particles.

Evidence that conflicts with the more "conventional" estimates of this new production has been presented recently (Schulenberger and Reid, 1981; Jenkins, 1982a). While there exists some controversy regarding the standard ^{14}C fixation methodology upon which the conventional views are based (e.g. Gieskes *et al.*, 1979;

1. Department of Chemistry, Woods Hole Oceanographic Institution, Woods Hole, Massachusetts, 02543, U.S.A.
2. Department of Biology, Woods Hole Oceanographic Institution, Woods Hole, Massachusetts, 02543, U.S.A.

Peterson, 1980; Williams *et al.*, 1983; Smith *et al.*, 1984), we feel that the more compelling evidence which raises concern about these production estimates is based on observations of tracer distributions. The attractiveness of tracer techniques lies in the fact that tracers tend to integrate over large space and time scales and as such provide representative averages of what are most likely heterogenous and sporadic processes. Determination of oxygen utilization rates (OUR) below the euphotic zone provides a useful estimate of new production in that the observed OUR must be stoichiometrically supported by a carbon flux from above. Determinations of OUR (Riley, 1951; Jenkins, 1977, 1980, 1982a) have been vertically integrated to yield carbon fluxes in pelagic waters of the order of 50 g C m^{-2} y^{-1}. This flux is about an order of magnitude greater than the production inferred using ^{14}C incubation techniques (e.g., Menzel and Ryther, 1960, 1961; Eppley, 1980) together with estimates of recycling efficiencies within the euphotic zone ranging from 80 to 90% (Eppley and Peterson, 1979; Harrison, 1980). Further evidence is accumulating (Jenkins, in preparation) that these OUR estimates are indeed realistic and accurate, but the magnitude of the disparity coupled with the importance of the issue compels us to seek independent evidence.

Evidence for higher productivity was suggested by Schulenberger and Reid (1981), who argued that the subsurface oxygen maxima that developed over periods of a few months between spring and summer within the seasonal thermocline of the mid latitude Pacific Ocean had to be of photosynthetic origin and represented a level of production that was large relative to that derived from ^{14}C estimates. These conclusions have been criticized on a number of grounds (e.g. Platt, 1984), principally on the question of spatial variability of the phenomenon. Nonetheless, the significance of the approach lies in the fact that, because such a large oxygen maximum is sequestered over a period of several months, the corresponding primary production must be *new*, not net. Any photosynthetically-fixed carbon that does not escape the euphotic zone ultimately must be oxidized, thereby removing the oxygen "signal." In consideration of the many factors potentially affecting the interpretation of this Schulenberger-Reid phenomenon, coupled with the promise of an independent determination of the rate of new production averaged over meaningful space and timescales (e.g. Jenkins, 1982a), we decided to examine the long term hydrographic and dissolved oxygen record available at the Panulirus site near Bermuda (Station S; see Jenkins, 1982b). The fact that this record extends over decades may give some confidence to the representativeness of our observations of seasonal trends in oxygen cycling, and at the same time begin to give insights into longer-term variations. Because Station S is within the "tight" recirculation region of the subtropical gyre (e.g., Worthington, 1976), it may be considered representative of a large oceanic area.

2. The Panulirus data

The Panulirus site, at 32N, 64W just south of Bermuda, has been occupied more than 500 times over an approximately thirty year period. The sampling frequency thus

corresponds to an average of about 3 weeks, and shows no pronounced winter/summer bias (Jenkins, 1982b), although sufficient year-scale gaps appear in the record. The data consisting of depth, temperature, salinity and oxygen were obtained from the hydrocast sheets and keypunched into a PDP 11 computer. No filtering or editing of the data was performed except to remove data that deviated by more than 3σ from the overall mean for a given density surface (Jenkins, 1982b). The data thus removed were less than 1% of the total, and did not significantly affect the overall means or trends. The oxygen data prior to 1961 were not included in the following analysis due to standardization problems associated with the pre-IGY analytical techniques (see Jenkins, 1982b). The record thus considered spanned 18 years from January 1961 to December 1978.

We concentrated our analysis on the upper few hundred meters. The standard sampling depths in this range were 1, 25, 50, 75, 100, 150, 200, 250, 300, 350, and 400 m. Examination of the deeper oxygen measurements, however, gives us an insight into analytical precision and systematic errors. Such measurements may be particularly sensitive to sampling problems due to the characteristically larger temperature difference between the samples *in situ* and the on-deck environment, and hence the greater risk of degassing due to warming. In addition, the longer time spent "on the wire" could exacerbate storage problems. The variance in the oxygen values thus obtained would represent an upper limit to measurement error inasmuch as some secular trend in salinity (Barrett, 1969) and oxygen at these levels has been observed (Jenkins, 1982b).

Block averaging the oxygen measurements at the 2000 (± 100) db level by month over the record yields a measurement variance of 0.125 ml/l for a given sample. This is somewhat larger than the 0.05 ml/l scatter expected for the "repeatability that can be achieved by a good analyst" (Carritt and Carpenter, 1966), but represents a variability accumulated over nearly two decades, with different analysts, standards, and equipment. The monthly oxygen means are not statistically different from one another (Table 1), although values obtained for the summer months (June–September) are $.031 \pm .010$ ml/l lower than during the winter months (November–April). This may be a sampling artifact due to exsolution caused by a greater degree of warming of the samples (either on the wire or on deck) in the summer months. From the viewpoint of examining seasonal trends, the uncertainty associated with a one-month record is .027 ml/l and for a seasonal (quarter year) mean, .016 ml/l. These uncertainties are very small relative to the magnitude of the variations reported here for the shallow waters.

3. The long term record

Before examining the oxygen record, we should look at the density structure. This stems from the recognition that the dissolved oxygen distribution observed at any point in the water column results from a combination of respiration, photosynthetic

Table 1. Monthly block averaged oxygen values at 2000 db for the Panulirus Station 1961–1978.

Month	Mean Oxygen (ml/l)	Variance (ml/l)	Number Observations	σm (ml/l)
January	6.039	0.122	16	.031
February	6.055	0.098	22	.021
March	6.073	0.112	22	.024
April	6.108	0.129	25	.026
May	6.137	0.141	22	.030
June	6.059	0.130	22	.028
July	6.041	0.154	28	.029
August	6.030	0.111	25	.022
September	6.015	0.106	22	.023
October	6.049	0.131	19	.030
November	6.054	0.152	23	.032
December	6.078	0.117	14	.031
Total (average)	6.062	0.125	282	.027

production (within the euphotic zone) and ventilation. By ventilation, we mean the imposition of surface layer characteristics (e.g. potential vorticity, near-saturation concentrations of dissolved gases) on the waters below the surface. The nature and magnitude of ventilation affects the distribution of density (via potential vorticity) and, in turn, is affected by it. The latter arises from the concept of the linkage between buoyancy flux and diapycnal turbulent diffusion (e.g. see Sarmiento *et al.*, 1976). Since secular variations in ventilation rates have been inferred to depths in excess of 500 m (Jenkins, 1982b), it is important to be aware of long-term changes in the density structure and hence the ventilation process. The density structure of the upper 200 m as a function of time from 1961 through 1979 shown in Figure 1, and other plots following, were objectively contoured using a standard two-dimensional spline fit routine.

The annual cycle of seasonal thermocline formation, intensification, erosion and ultimate destruction is clear from the record. What is noteworthy, however, is the long-term behavior of the $\sigma_\theta = 26.2$ isopycnal. Throughout the 1960s it executes a cycle of deepening to 100 or 150 m throughout the year, followed by shoaling and occasionally surfacing in late winter (February to March). Beginning in 1972, however, this isopycnal deepens persistently to about 200 m in 1976, not shoaling above 100 m until the winter of 1977–1978. The $\sigma_\theta = 26.4$ isopycnal also follows this trend, in that it only shoals above the 200 m level from 1964–1972. In fact, this overall trend is observed in those isopycnals spanning the entire top 600 m. This is underscored by salinity, oxygen and depth correlations which indicate that water-mass formation and ventilation were less vigorous during the mid 1970s, while the mid 1960s and late 1970s were periods of more vigorous renewal. For example, the ventilation timescale (i.e., the

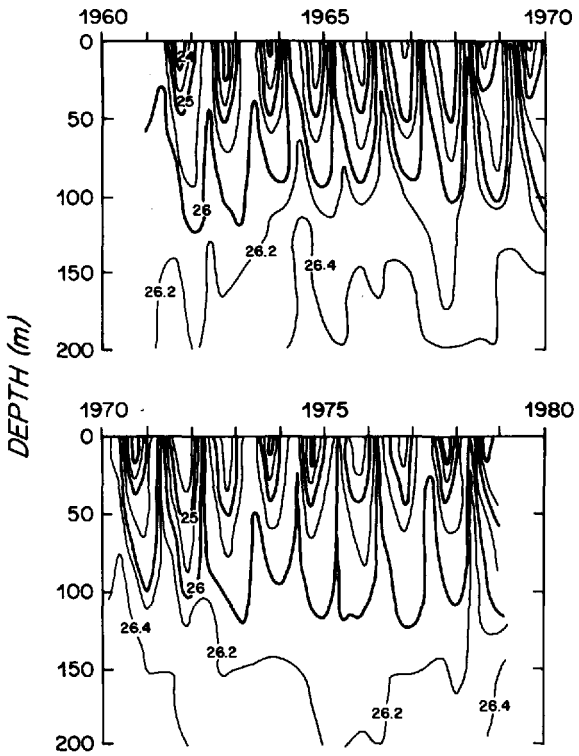

Figure 1. The Panulirus Potential Density Record (1961–1979). Note the deep penetration of the 26.2 contour during the mid-1970s, along with the "disappearance" of the 26.4 contour.

box-mixing residence time—see Jenkins, 1980) for the σ_θ = 26.40 surface in the mid-seventies was twice that in the mid-sixties (Jenkins, 1982b).

Bearing this observation in mind, we turn to the oxygen record (Fig. 2). We present the oxygen data as ΔO_2, excess above solubility (solubility estimated using the equation derived by Weiss, 1970); i.e., as negative A.O.U. in ml/l. The seasonal cycle is clear in the 1960s, particularly when one observes the zero ΔO_2 contour. The zero line rises to the surface in late winter, and deepens to about 100 m during the latter part of summer. Peak values occur at about 50 m, and are about 0.4 to 0.5 ml/l above saturation. These oxygen excesses we conjecture (as did Schulenberger and Reid, 1981) to be a result of photosynthetic activity. Their subsequent erasure is due to wind induced and convective mixing processes. During the mid-1970s there is, however, a deepening of the zero line, and the creation of even larger excesses. We suggest that this is a result of poor ventilation during that period, with the re-establishment of the "normal" cycle only occurring during 1978. We were fortunate to have a comparison of ^{3}H-^{3}He characteristics between 1974 and 1978, which clearly shows the dramatic differences in ventilation (Jenkins, 1982b, Fig. 8) between these two times.

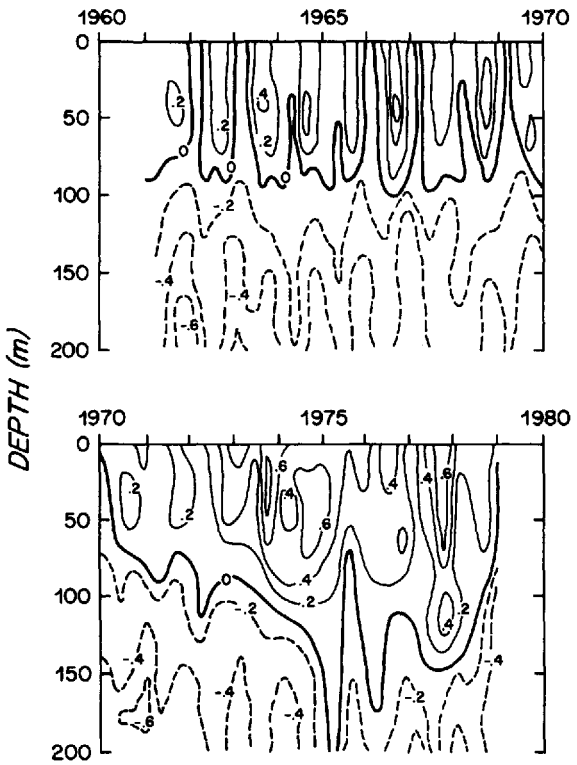

Figure 2. The Panulirus Oxygen Anomaly Record (1961–1979). The oxygen anomaly is defined as the supersaturation in ml/l. Note the strong seasonal cycle of the 1960s, and its subsequent confusion during the 1970s: the 0 ml/l contour dives below 100 m in 1973–74 due to inefficient removal of the photosynthetic oxygen.

The integrated ΔO_2 for the upper 100 m (ΣO_2) vs. time, expressed in $lO_2\ m^{-2}$, i.e. the amount of oxygen produced in a column of water 1 m × 1 m by 100 m high is shown in Figure 3. The seasonal cycle in ΣO_2 is evident, especially in the 1960s, and is characterized by minima and maxima during late winter and midsummer respectively. As expected, there appears a longer term secular increase in ΣO_2 during the mid-1970s, coupled with some disturbance of the seasonal cycle (although still present), followed by a re-establishment of the "norm" in 1978. The muddling of the seasonal signal during the poorly ventilated years is not unexpected, as the erasure of the oxygen maximum is not accomplished effectively. The nature of our analysis, i.e., the cutting off of integration at 100 m, leads to an underestimate of the positive secular swing in ΣO_2 because, as can be seen in Figure 2, the zero ΔO_2 line penetrates well below that depth during that period. Because of the anomalous character of the mid-1970s, we choose to analyze only the period 1961–1970. It can be shown (and can be qualitatively seen from Figs. 2 and 3) that the seasonal variations, when corrected

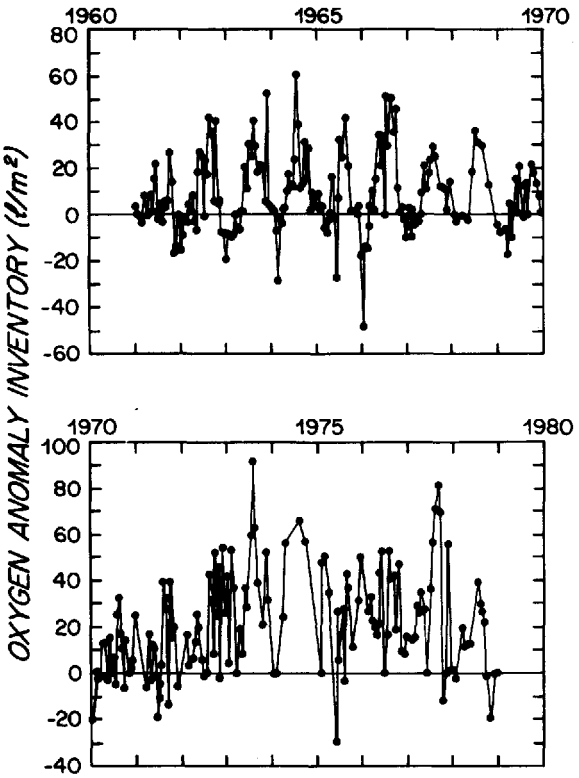

Figure 3. The Integrated (0–100 m) Oxygen Anomaly Record (1961–1979). Note the clear seasonal signal throughout the 1960s and the lower frequency (interannual) upward shift through the 1970s.

for secular interannual trends, are essentially the same but somewhat noisier for the latter period. It will also be seen that considering some of the more fundamental questions that need to be asked, the inclusion of the larger data set is not really justified, and that we learn more by examining the "cleaner" part of the record.

4. Seasonal cycles

The average (1960–1970) seasonal cycles in density and ΔO_2 are shown in Figures 4(a) and (b). The stations for this period were simply binned by julian day and objectively contoured via a two-dimensional spline fit algorithm. The data in this figure and subsequent ones are repeated for 6 months either side of the annual span to show the cycles more clearly. The formation and destruction of the seasonal thermocline is the dominant feature in the density cycle, and it is characterized by the appearance, deepening and abrupt disappearance of the $\sigma_\theta = 26.0$ isopycnal. Stratification begins in spring (April–May) and intensifies until late summer (August–September), after

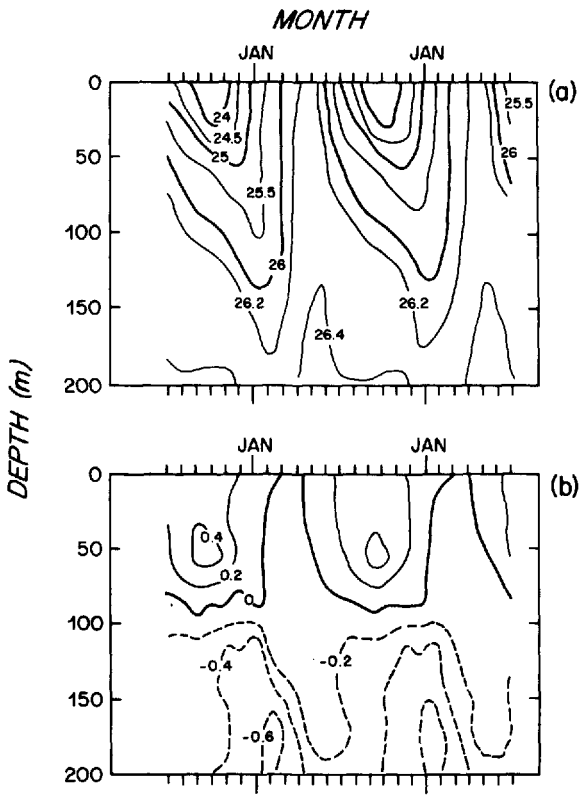

Figure 4. (a) Average Seasonal Density Cycle (1961–1970). (b) Average Seasonal Oxygen Anomaly Cycle (1961–1970). Note the mirror-like behavior in the aphotic zone due to oxidation of the carbon rain.

which the erosion of the thermocline is seen in the rapid rising and disappearance of many of the isopycnals. Extensive vertical mixing occurs in the latter part of winter (February–March, as discussed, for example, by Warren (1972)).

The ΔO_2 record changes with the density field in a consistent way. ΔO_2 begins to accumulate in early spring, reaching a maximum in late summer with the stratification, and then eroding gradually until late winter mixing erases it completely. The effect of surface forced gas exchange is clear in the tendency for the maximum to deepen from August through November, with the ΔO_2 isopleths approaching the vertical and paralleling isopycnals. The slight ΔO_2 residual near the surface in January is interesting, and it is tempting to speculate that it may be a result of new production spurred by the vertical flux of nutrients brought on by vertical mixing. An additional contributing factor would be the finite impedance to gas exchange.

The most striking feature of the ΔO_2 record, however, is the mirror-like behavior in the deeper water: the ΔO_2 maximum at about 50 m is mirrored by a minimum (AOU maximum) more than 100 m below (Fig. 4). Equally interesting is the fact that the

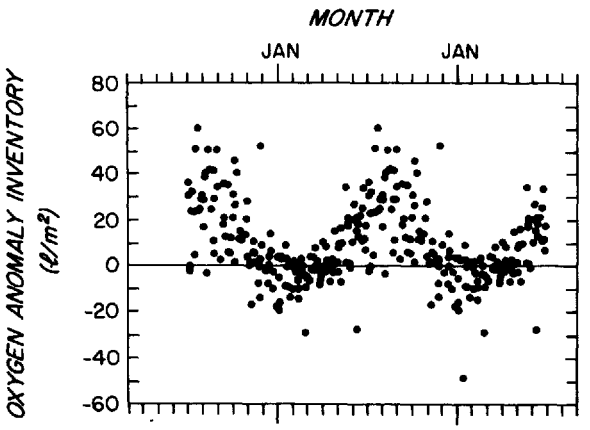

Figure 5. The Mean Seasonal Integrated Oxygen Anomaly trend (1961–1970).

deeper signal lags the shallower one by two to three months. We suggest that the deep water variations are induced by oxidation of carbon fixed above by photosynthetic activity. The amplitude of the variations (see below) is consistent with this hypothesis. The lag, at first glance, is likely not due to the downward transit time of particles, because typical sinking rates are too fast. A more likely explanation of the observed lag is that photosynthetic oxygen production (and hence carbon fixation and particle flux) continues throughout the year, but the destruction of the seasonal thermocline prohibits the accumulation of the shallow oxygen signature. The increased vertical mixing in the latter part of the autumn thermocline erosion process would be expected to bring deeper nitrate to the euphotic zone, and hence spur increased photosynthetic activity, leading to greater oxygen consumption rates below.

An additional contributing factor to the lag in the deeper waters may result from lateral ventilation processes. Examination of the oxygen and density records indicates that local vertical ventilation occurs only to about 100 to 150 m depth. Below this depth, ventilation must occur laterally on isopycnals (Jenkins, 1980). Increasing depth is characterized by distances to the outcrop regions and decreasing horizontal velocities, so that appreciable time lags are observed for deeper isopycnals (see Jenkins, 1982b): 1–2 months for σ_θ = 26.4 (average depth = 225 m) and 2–3 months for σ_θ = 26.5 (average depth = 340 m). The observed lag, however, is clearly larger than this trend would predict, so we must conclude that it results from early destruction of the shallow maximum due to vertical mixing and ventilation. The oxidation signal, on the other hand, continues to build up all year.

Inspection of the seasonal ΣO_2 trend for 1961–1970 (based on data in Fig. 3) (Fig. 5) suggests that the minimum in January through March is due to vertical mixing of oxygen-depleted waters from below with inadequate time for gas exchange equilibrium with the atmosphere. The apparent increase in the six months is about 40 lm^{-2} (1.8 M m^{-2}). It is not inappropriate to extrapolate this estimate over the entire year;

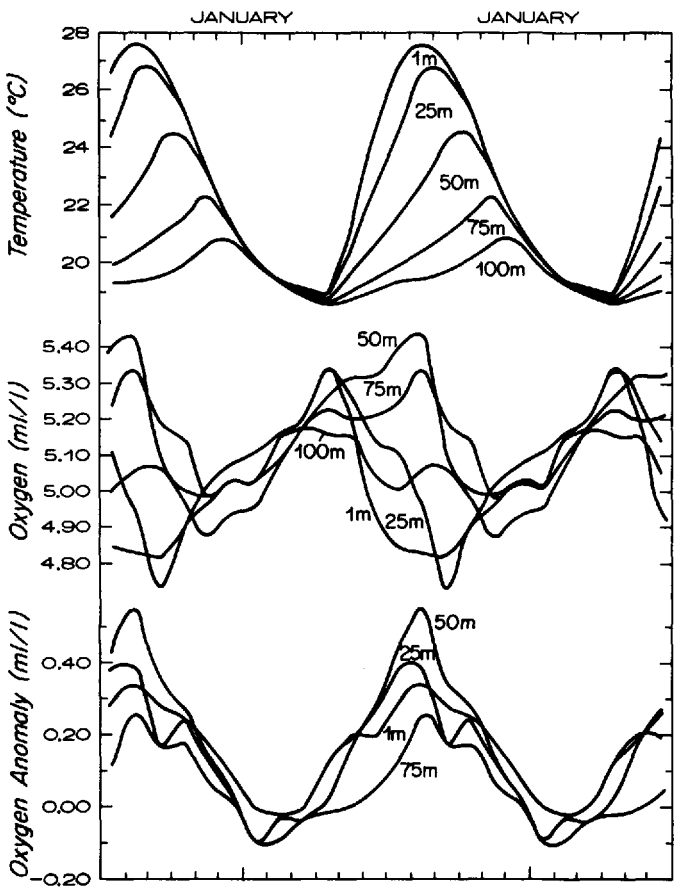

Figure 6. Shallow mean seasonal trends in temperature, dissolved oxygen and oxygen anomaly (1961–1970).

since it spans a time (June–August) considered by many to be a time of minimal productivity (e.g. see Menzel and Ryther, 1961), giving an annual oxygen production of 80 lm^{-2} (3.6 M m^{-2}). Clearly, however, the possible loss of oxygen by gas exchange makes this a minimum estimate.

The seasonal cycles of temperature, oxygen and ΔO_2 are shown in Figure 6 for 4 depths (1, 25, 50 and 75 m) for 1961–1970. Oxygen concentrations, at least for the shallowest depths, will be influenced by gas exchange and the seasonal temperature cycles, through the temperature dependence of solubility. The vertical homogeneity of these surfaces is evident from January through March, where all records tends to overlap. The continued decrease in temperature through this period is mirrored by an oxygen increase—an effect driven by vertical convection and ventilation. Remarkably, ΔO_2 actually decreases during the initial part of the record (December–January) becoming negative before gradually increasing to positive values again in March–

April. This clearly is an artifact of a finite gas exchange impedance felt by oxygen. From radon measurements the equivalent stagnant film thickness has been estimated to be about ~40 μ (Peng *et al.*, 1979), giving an oxygen piston velocity of about ~5 m d^{-1}. This implies a gas exchange timescale of about 20 days for a 100 m vertical mixing layer, consistent with the idea that vertical mixing of negative ΔO_2 water from below can depress the overall ΔO_2 below zero before gas equilibration can catch up. This impedance is further evident in Figure 4(b) where it is shown that the nearly 100 m depression of the -0.2 ml l^{-1} ΔO_2 isopleth does not occur until March.

When stratification begins in April, the oxygen records immediately diverge, and there is an immediate increase of 0.10 ml l^{-1} in the 1 m and 25 m oxygen curves before decreasing due to gas exchange. This increase corresponds to a production of more than 50 mg C m^{-3} d^{-1}. The net increase in oxygen at 50 m between March and July is nearly 0.20 ml l^{-1}. With the exception of the first month when the 25 m level oxygen slightly exceeds the 50 m level, this layer represents a maximum in the vertical distribution of oxygen; hence, there is no way except by photosynthesis for the absolute oxygen concentration at this level to increase. This increase represents an absolute lower limit of 15 l O_2 m^{-2} y^{-1} to the level of photosynthesis since vertical mixing both above and below serve to remove this oxygen. As we will attempt to demonstrate, this lower limit is much smaller than the true rate or production.

The ΔO_2 curve for 50 m reaches a maximum of nearly 0.5 ml l^{-1}, before decreasing. Both vertical and isopycnal exchange processes will tend to reduce this maximum, both because the absolute oxygen concentrations elsewhere are lower, and because the degree of supersaturation at this depth exceeds that of the other strata. There may be a small tendency to increase ΔO_2 by mixing due to the curvature of the solubility as a function of temperature, but this is negligible in this case. Isopycnal processes will also reduce ΔO_2, inasmuch as outcropping will present an upslope negative gradient due to gas exchange, and a downslope negative gradient below the euphotic layer.

Radiative heating may also contribute to the signal: warming the water without gas exchange will generate an apparent supersaturation. To assess the importance of this process, we need only to make the distinction between radiative and nonradiative heating. We attempt to show that the seasonal temperature increase at the depth of the oxygen anomaly maximum (50 m) is far larger than that expected from irradiation alone. The ultimate source of this heat is a combination of shallow irradiance, latent and sensible heating at the surface combined with downward mechanical mixing.

Using Paulson's and Simpson's (1977) reformulation of Jerlov's (1968) irradiance profiles for type IA waters (appropriate for this area), and recognizing that the rate of radiative heating is obtained from

$$\frac{(\partial\theta)_I}{\partial t} = \frac{\partial I}{\partial z}$$

$$I = RI_o e^{Z/\zeta_1} + I_o (1 - R) e^{Z/\zeta_2}$$

leads to the following expression

$$\frac{(\partial\theta)_I}{\partial t} = I_o\left[\frac{R}{\zeta_1}e^{Z/\zeta_1} + \frac{(1-R)}{\zeta_2}e^{Z/\zeta_2}\right]$$

For type IA waters, we have $R = 0.62$, $\zeta_1 = 0.60$ m and $\zeta_2 = 20$ m, and using a mean surface irradiance of 430 cal cm^{-2} d^{-1} for the period March through July, we obtain a radiative warming of 0.75°C. Alternatively, using Ivanoff's (1977) graphically presented irradiance curve (his Fig. 5.16) a somewhat greater increase of 1.0°C is obtained. This is clearly an oversimplification of the problem because we have assumed that lateral advection of heat can be ignored. Prangsma *et al.* (1983), however, have obtained a satisfactory heat balance with a one-dimensional model provided that the data are averaged over length scales larger than the mesoscale. Here we rely on time averaging to smooth out lateral advection of mesoscale variability, and the relative smoothness and reproducibility of the seasonal cycle suggests we are not grossly in error.

It is noteworthy that the observed mean seasonal temperature change at 50 m is 6°C (Fig. 6), far greater than that predicted from radiative heating alone. First, this means that direct insolation can account for only about 20% of the observed ΔO_2. Second, the fact that the temperature rise is far larger than the radiative heating implies that the bulk of the heat transported to this depth is by turbulent (mechanical) exchange. This is consistent with currently successful mixed-layer models, which attribute the bulk of heat transport at the base of the mixed layer to mechanical (current) shear (e.g. Klein and Coantic, 1981; Mellor and Durbin, 1975). This in turn implies that a reciprocal (upward directed) flux of the photosynthetically produced oxygen must occur. A crude estimate of the loss of oxygen can be made as follows. The mean volumetric thermal gradient ($\rho\, C_p\, \Delta T/\Delta Z$) between 25 and 50 m is of the order of 0.1°C/m or 10^5 cal m^{-4}, and the mean oxygen gradient is about 10 ml m^{-4} (450 μM m^{-4}) above the 50 m maximum and 6 ml m^{-4} (270 μM m^{-4}) below it. The observed seasonal heat storage below 50 m corresponds to a thermal flux of approximately 250×10^6 cal m^{-2} y^{-1}, giving an upward oxygen flux of roughly 1 M m^{-2} y^{-1} and a downward flux of about 0.7 M m^{-2} y^{-1}. Combined with the oxygen excess actually accrued over the period (April to August), this leads to an annual oxygen production of approximately 5 M m^{-2} y^{-1}.

Based on the above flux calculation it is evident that most of the oxygen produced is not sequestered, but escapes upward. The downward flux component, about 1 M $m^{-2}y^{-1}$ is also very large, and as will be seen in the next section, significant for the deeper budgets. Hence, by examining the temperature evolution, it appears that the observed sequestering of oxygen is but a remnant of the actual production. In Section 6 we present additional data as to how leaky the system may be, but in the next section we examine the deeper oxygen record for further constraints on the downward flux of carbon.

5. The deeper oxygen cycles

Ventilation of the deeper (>100 to 150 m) strata occurs elsewhere, and only in late winter (e.g. see Worthington, 1959; Stommel, 1979); yet, the shallow subsurface oxygen buildup, suggests that the rain of particulate carbon from the euphotic zone occurs at various rates throughout the year. If the oxygen consumption rates obtained from transient tracers (Jenkins, 1977, 1980, 1982a) are accurate, i.e. that from 0.1 to 1 ml l^{-1} y^{-1} are consumed in the upper few hundred meters, then one should see a measurable annual oxygen cycle consisting of ventilation (a sharp increase) followed by consumption (a gradual decrease).

The photosynthetic increase seen in the shallow (<100 m) curves is mirrored in the deeper layers, as evident in plots of the mean (1961–1970) annual trends for oxygen at depths ranging from 100 to 400 m (Fig. 7). Here ΔO_2 is used to separate the curves by depth, although the equivalent oxygen curves could be used since temperature is essentially constant in time. At 100 m the curve begins to reverse in tendency, decreasing after the later winter maximum in association with the convection period (mid-March). There is considerable statistical noise in the record at 100 m, most likely due to secular variations in penetration of the $\Delta O_2 = 0$ isopleth (see Fig. 2) and due to competition between oxidation and photosynthesis. Below this depth the amplitude of variation is much greater. Allowing that the 100 m record is transitional, we see below 150 m a decreasing amplitude and increasing lag with depth. The former is clearly due to the exponentially decreasing oxygen consumption rates (cf. Jenkins, 1980, 1982a) and decreasing ventilation rates (Jenkins, 1980). The latter is a result of increasing distances from outcrops (Jenkins, 1982b). The amplitudes of the oxygen cycle at each depth, as obtained by the difference between the means of the three contiguous maximum and the three contiguous mininum monthly values (Table 2), are plotted in Figure 8.

It must be recognized, however, that the above flux is an underestimate for three reasons. First, the oxygen decrease appears to occur over an eight or nine month period, and is masked by the ventilation process for the remainder of the year. The above estimate may thus be low by about 30%; i.e., the fraction of time during which the potential oxygen decrease is overcome by the horizontal influx of oxygen from late winter ventilation processes. Also in Table 2 is the estimated oxygen consumption rates obtained by extrapolating the observed oxygen changes over the full year. The values thus obtained are consistent with OUR determinations made with $^3He/^3H$ dating (Jenkins, 1977, 1980) for this area. An integration of the OUR between 100 and 400 m here yields an equivalent oxygen consumption flux of 4.1 M m^{-2} y^{-1}.

Second, we have ignored consumption deeper than 400 m. A simple linear extrapolation of the trend would augment the flux by as much as 8%, whereas a logarithmic extrapolation based on a least squares fit to the data

$$\ln A = -0.53 - Z/264 \text{ m}$$

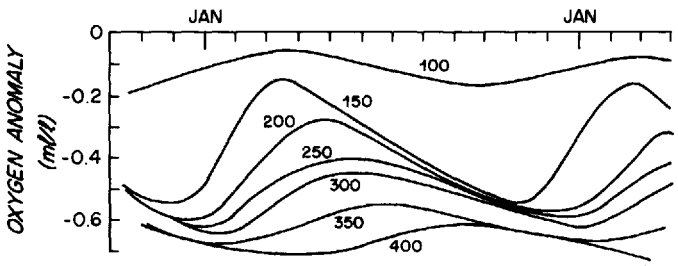

Figure 7. Deeper mean seasonal oxygen trends (1961–1970). Note the decreasing amplitude and increasing lag with depth.

increases the sum as much as 50%. Although the fit is moderately good (broken line in Fig. 8), such an extrapolation of the seasonal oxygen amplitude (A) is not to be viewed with any confidence. We are left with the intuitive statement that the amount of oxygen consumed below 400 m lies between 0.25 and 1.5 M m^{-2} y^{-1}.

Third, a downward flux of photosynthetic oxygen will reduce the amplitude in the shallower strata (i.e., at 100–150 m). That such a flux occurs is implied by consideration of the nitrogen cycle (Section 8): the upward flux of nitrate by turbulent exchange processes which must fuel the new production will be reciprocated by a downward flux of oxygen. The vertical gradient of oxygen is about 130 n M m^{-1} at

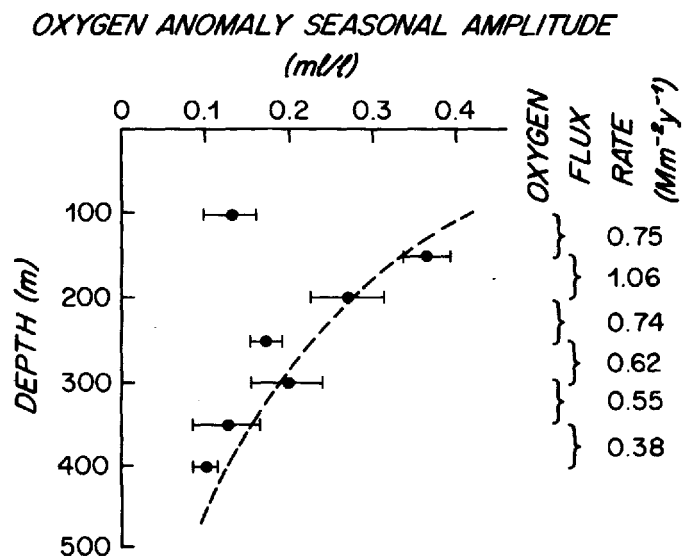

Figure 8. Aphotic zone oxygen respiration cycle amplitudes vs. depth (see Fig. 7). The broken line is the logarithmic fit to the data (see text) and the numbers to the right are the annual consumption of oxygen in moles m^{-2} for the depth interval spanned by the two adjacent (above and below) data points.

Table 2. Amplitudes of seasonal variations in oxygen concentrations below the euphotic zone, and their implied oxygen utilization rates.

Depth (m)	Seasonal Amplitude (ml/l)	Estimated OUR (ml/l/y)
100	0.13 ± 0.03	—
150	0.36 ± 0.03	0.54
200	0.26 ± 0.05	0.39
250	0.17 ± 0.025	0.26
300	0.20 ± 0.04	0.31
350	0.13 ± 0.035	0.20
400	0.10 ± 0.02	0.15

100 m in mid season, and nitrate is about 60 nM m^{-1}. An upward flux of roughly 0.6 M(N)m^{-2} y^{-1} would be required to support the carbon rain, implying a corresponding downward oxygen flux of 1.3 M m^{-2} y^{-1}. This calculation at first seems tautological, in that we assume a carbon flux to estimate the nitrate and hence oxygen flux, ultimately to calculate the carbon flux. However, it should be realized that this procedure is perturbative, leading to only a 20 or 30% increment in the final result. Moreover, the magnitude of this downward oxygen flux is roughly consistent with the heat budget normalized flux obtained above.

Some fraction of the observed annual cycle of oxygen in these layers ultimately will be due to ventilation-mixing alone. That is, proximity to the ventilation regions makes the local impact of ventilation large, and there will be a subsequent reduction in oxygen content as the ventilated water is mixed into the interior. Consideration of the inter-annual and annual salinity and oxygen records suggests that this effect accounts for no more than 25% of the observed seasonal slope in oxygen (see Jenkins, 1982b). Here we take the conservative tactic of reducing the integrated oxygen flux estimates by this amount.

In summing up, by considering the deep oxygen cycles, we arrive at an estimated oxygen consumption rate of at least 4.1 M m^{-2} y^{-1}, and as much as 5.9 M m^{-2} y^{-1}, depending on the mode of extrapolation to deeper strata. This leads to an estimate of new production of 40 to 57 g C m^{-2} y^{-1}. It is entirely consistent with earlier estimates (Jenkins, 1982a) based on transient tracer calibrated OUR data. It is encouraging that the two differing approaches, i.e. the transient tracer and annual cycle estimates, yield essentially the same values.

6. Tritium-^{3}He dating

The *in situ* production of ^{3}He by the decay of nuclear weapons-produced tritium provides a chronology on timescales of 0.1 to 10 years which can be used for looking at the rates of processes in the sea (see, e.g. Jenkins, 1980, 1982a). Late winter convection and mixing (February–March) nearly zeros the ΔO_2 in the upper 100 m, and due to the greater mobility of helium, one expects that the ^{3}He/^{3}H clock will be even more

effectively zeroed. As will be seen, any slight remnant age will, in fact, make our estimates more conservative.

Vertical profiles of $^3He/^3H$ age, dissolved oxygen, ΔO_2 and σ_θ for a station taken at the Panulirus site on August 15, 1978 are shown in Figure 9. The time of sampling corresponds to the seasonal peak in the oxygen maximum (Figs. 6, 7) and thus represents the accumulation of both photosynthetic oxygen and tritiugenic ^3He *in excess of that which is lost* by upward gas exchange with the atmosphere over approximately 5 months. Although helium has a molecular diffusivity greater than that of oxygen, and hence may exchange more quickly with the atmosphere, the existence of strong vertical gradients in oxygen above 50 m indicates that the primary impedance to gas exchange for oxygen during this time is not at the boundary layer, but rather in vertical transport within the water column. Further, vertical mixing with deeper waters (below 50 m) will transport ^3He upward and inflate the $^3He/^3H$ age, yet transport oxygen downward and decrease the oxygen excess.

The subsurface oxygen maximum (here corresponding to a supersaturation of 0.42 ml l^{-1}) is clearly evident at 50 m; yet the average $^3He/^3H$ age in the upper 50 m is 0.05 ± 0.08 y, i.e. not significantly different from zero, and much less than the chronological age of about 0.42 years. This, of course, is consistent with the downward mechanical mixing of heat (see Section 4), and further allows us to argue that *at least* 70% of the ^3He and hence a similar fraction of oxygen has been lost upward over this time. Considering the degree to which ^3He has been lost (the $^3He/^3H$ clock is not significantly different from zero), and considering the presence of strong mechanical mixing, it is not inappropriate to use the saturation anomaly in oxygen, viz. ΔO_2, as a minimum measure of the evolved oxygen. This points to a minimum oxygen production of nearly 2 moles per square meter over that period, corresponding to an average productivity of about 4.5 M m^{-2} y^{-1}. In this calculation, we have not accounted for the downward flux of oxygen or the productivity below 50 m, both of which are undoubtedly significant as suggested in the previous section.

The $^3He/^3H$ age of 1.0 y at 95 m suggests that the deeper vertical flux of ^3He, and hence of oxygen, must occur. The depth is shallow enough to be reached by vertical mixing during the late winter: the hydrographic record indicates that this particular density surface (σ_θ = 26.0) actually surfaced the previous winter; and late winter $^3He/^3H$ data (Jenkins *et al.*, 1979) indicate that age is "zeroed" to 150 m. The existence of a $^3He/^3H$ age of about double the chronological age requires a significant upward transport of ^3He, and by inference, a downward flux of oxygen. This is consistent with the temporal ΔO_2 trends below the euphotic zone discussed in the previous section, but to quantify the fluxes would require a model calculation for which the appropriate $^3He/^3H$ data do not at present exist. We can, nonetheless, suggest that the downward flux of oxygen significantly reduces the observed inventories, making our production estimates a lower limit.

On the other hand, we have neglected the apparent supersaturation which is

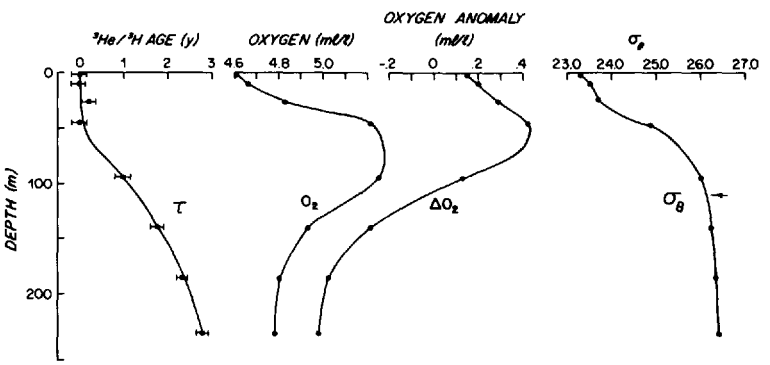

Figure 9. Profiles of $^3He/^3H$ age, dissolved oxygen, oxygen anomaly and density for a station taken at the Panulirus site on August 15, 1978. The arrow points to the depth of the climatological mean wintertime outcrop density, and the minimum depth to which ventilation occurred the previous winter.

generated by the presumably higher interfacial impedance gas exchange compared to heat transfer. That is, the warming of waters by insolation and mechanical transfer outpaces the ability of the water column to reach oxygen solubility equilibrium, thereby producing a tendency to supersaturation. As will be discussed in the next section, the subsequent oxygen "unloading" produces significant surface outfluxes, but only amounting to a fraction (order one third) of the apparent productivity. Examination of the seasonal oxygen records, also show substantial vertical gradients in oxygen in the upper 50 m during the summer months. If gas exchange were the rate limiting process, i.e. sufficiently slow to generate the observed supersaturations, one would expect the upper 50 m to be relatively homogeneous, with the vertical gradient concentrated in the top few meters. As this is not the case, the observations support a strong *in situ* source of the oxygen supersaturation, rather than physical-kinetic effects. Crudely, the above concerns again lead to an estimate of the order of 5 moles $O_2\ m^{-2}\ y^{-1}$.

7. Gas exchange fluxes

It is especially evident in Figure 6 that throughout the bulk of the year (April through December) the 1 m depth is supersaturated. Broecker and Peng (1982) pointed out that surface water oxygen concentrations measured on the GEOSECS expedition were on the average 3% above saturation, so this is not an isolated phenomenon. The existence of such a supersaturation implies a flux of oxygen to the atmosphere which must be supported by *in situ* production. It is of interest to use what we know of gas exchange rates to estimate the magnitude of these fluxes and thereby constrain the *in situ* production rates. As will become evident in this discussion, however, the constraints thus obtained are exceptionally crude due to the lack of the

necessary quantitative gas exchange data. But, it is worthwhile to explore this approach to point out how, when and where such data will be needed to make a more refined calculation.

An initial calculation can be made on the basis of the Broecker and Peng observation. Crudely, an observed oxygen supersaturation of ~0.15 ml l^{-1}, coupled with a gas exchange rate of about 4 m d^{-1} [using the GEOSECS global Rn evasion results of Peng *et al.* (1979), and scaling the piston velocity according to $(Do_2/D_{Rn})^{1/2}$] yields an evasion rate of more than 10 moles O_2 m^{-2} y^{-1}. This is clearly an overestimate, since both estimates are mean values, and the oxygen supersaturation should be inversely correlated with gas exchange rates. To contend with this, we must incorporate the seasonal variations in gas exchange rates and oxygen anomalies into our calculation. Direct (Rn) gas exchange rates for this region are few in number and do not systematically span the seasonal cycle. Consequently we must rely on wind-tunnel data to estimate exchange rates.

The primary difficulty with applying wind tunnel data to natural systems lies in the effects of a finite fetch, and the nonrepresentativeness of wave spectra. Jahne *et al.* (1979) have successfully circumvented the former problem by using a circular wind tunnel, generally achieving lower gas exchange rates as a function of friction velocity than more conventional wind tunnel studies (e.g. cf. Broecker *et al.*, 1978; Liss, 1973). Such results should be related to oceanic ^{222}Rn experiments but a detailed comparison is made difficult by the apparent lack of strong correlation between "instantaneous" (24 hr) wind speed and Rn evasion rate (Peng *et al.*, 1979). This lack of correlation is likely due to the longer term integrating effect of Rn (λ^{-1} = 5.5 days) and to the lateral advection of heterogeneities. In general, the Jahne *et al.* results predict lower piston velocities than those observed during GEOSECS (compare Peng *et al.*, 1979, Fig. 12a with Jahne *et al.*, 1979, Fig. 2 for the lower wind speeds), and the "climatological mean" gas exchange rates (Broecker and Peng, 1982). Part of this may be due to the limitations of wave height and spectra within the wind tunnel, and part may be due to enhancement of gas exchange in the natural environment by wave-induced bubbles (e.g. see Atkinson, 1973; Hasse and Liss, 1980). Hence the Jahne *et al.* exchange rates are probably a lower limit to the true exchange rate, and thus a conservative estimation of the oxygen fluxes calculated below (Deacon, 1981).

We use the N_2 evasion data from Jahne *et al.* (1979), according to the relation

$$V_p(N_2) = 0.142\,V_w + 0.24 \qquad 0 \le V_w \le 7 \text{ m s}^{-1}$$

and

$$V_p(N_2) = 9.354\,V_w - 64.25 \qquad 7 < V_w < 12 \text{ m s}^{-1}$$

where V_p is the nitrogen piston velocity in m d^{-1} and V_w is the wind speed in m s^{-1}. To convert to oxygen piston velocities we use the relation

$$V_p \alpha \left(\frac{D}{\nu}\right)^{1/2}$$

at constant friction velocity, and we use the molecular diffusivities obtained by Wise and Houghton (1966)

$$D(O_2) = 0.0338\, e^{-2.146/T\times 10^3}$$
$$D(N_2) = 0.437\, e^{-2.857/T\times 10^3}.$$

Wind data are taken from a compilation by Bunker and Goldsmith (1979) for the period 1961–1970 in Marsden Square 115. The mean winds thus obtained were scaled down by a factor of 0.91 to accommodate for the characteristically lower winds in the Bermuda section of the Square. This factor was obtained by comparison with the longer term mean winds for the smaller area bounded by 32–34N and 60–70W. This is a conservative estimate in that the advection of surface waters tends to bring in water from the more northerly and hence windier parts of the Square. Further, bearing in mind the strong change in slope of V_p vs. V_w at 7 m s^{-1} wind speed, climatological averaging of winds when near this critical velocity will tend to underestimate V_p, also making this a conservative estimate of gas fluxes.

The seasonal cycles in the wind velocity, piston velocity, excess oxygen (at 1 m depth) and the computed flux of oxygen to the atmosphere are summarized in Figure 10. The most prominent features of the oxygen flux curve are the two maxima (spring and fall) and the negative excursion during late winter. The spring maximum is consistent with high levels of photosynthesis at that time, but the autumn maximum is enhanced by the fall mixed layer deepening and hence in part results from the subsequent unloading of the photosynthetic oxygen sequestered through the summer as well as enhanced productivity due to nutrient recycling. It is important to note that these maxima result from the interaction between changing ΔO_2 and V_p, and hence appear somewhat circumstantial. However, their consistency with both the known biological cycling and observed changes in water column oxygen inventories is compelling.

Integration of the curve from March through January yields a net flux of 6.9 M (O_2) m^{-2} y^{-1}. The fact that this is not apparently balanced by an influx during the January–March period is not surprising in that the ingassing process is storm event driven, and related to convective mixing. This kind of process is not amenable to simple theory and measurement. It does, however, underline the uncertainties of this kind of calculation.

In estimating the total efflux of oxygen, we must account for the unloading of mixed layer oxygen due to thermally driven solubility changes. That is, what fraction of this outgassing flux can be attributed to the simple physical effect of exsolution due to warming? This is difficult to estimate because a significant fraction of the water column never reaches solubility equilibrium except during the late winter. However, we can obtain an upper limit to the exsolution unloading flux by simply taking the difference between the maximum solubility equilibrium oxygen inventory in the upper 100 m (23.2 M m^{-2} during March), and the minimum (21.2 M m^{-2} during August).

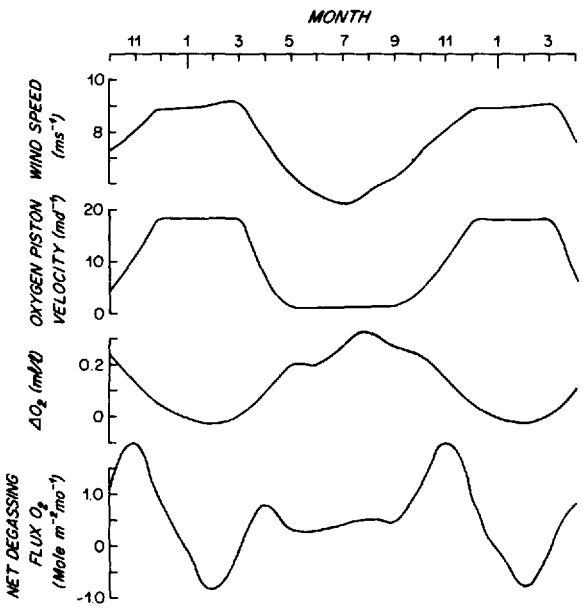

Figure 10. Seasonal cycles of wind speed, computed oxygen piston velocity, measured oxygen anomaly at 1 m and estimated oxygen outgassing flux.

The difference, 2.0 M m^{-2}, represents a firm upper limit to the exsolution flux, because the upper 100 m of the water column are generally supersaturated (after March) and hence does not achieve its full outgassing flux. The above permits us to obtain a crude, but conservative estimate of the biogenic oxygen flux of about 5 M m^{-2} y^{-1}.

8. Nutrient fluxes

New production must be supported by an upward supply of nutrients. Previously, this upward nutrient flux has been estimated using observed mean vertical gradients through the seasonal thermocline and "reasonable" turbulent diffusion coefficients (e.g., see McCarthy and Carpenter, 1983; Platt *et al.*, 1984). The difficulty of this approach is that the assumptions implicit in such a parameterization are clearly inappropriate, largely due to strong ocean-atmosphere dynamical coupling, the short timescales associated with both the turbulent transport of nutrients and their utilization, and the unsteadiness associated with thermocline erosion and mixed layer evolution. Further, the flux of nutrients must be event-dominated and hence difficult to contend with in such a simplified model. That is, periods of intense wind activity will tend to promote vertical mixing and enhance the upward flux of nutrients. These periods may, in fact, be responsible for much of the transport of nutrients, and bear little relationship to the "mean state."

One-dimensional, time-dependent, mixed-layer models appear to be moderately

successful in simulation of thermocline-mixed layer evolution and heat budgets (e.g. see Prangsma *et al.*, 1983; Klein and Coantic, 1981), and represent a significant improvement over the one-dimensional diffusion models. What is particularly interesting is that the second order turbulence closure models used by Klein and co-workers do not use adjustable parameters, lending some degree of confidence to the nutrient fluxes obtainable from such a model. Klein and Coste (1984) have computed nitrate transport through the seasonal thermocline for three locations in oligotrophic waters, using such a model with real-time wind and thermodynamic forcing. Estimated fluxes of nitrate were extremely variable and pulse-like, even with (artificially) constant wind stress. The potential impact of this periodic nutrient flux on the long-term nutrient budget in the euphotic zone is dramatic compared to what might be expected from estimates based on a simple vertical diffusion model. For example, when these short-term fluxes are integrated over a full year for one location, the western Mediterranean Sea, the total flux of NO_3^- across the thermocline is ~0.9 M m^{-2} y^{-1} (Klein and Coste, 1984). This input of nitrogen corresponds to *new* primary production of ~70 g C m^{-2} y^{-1}, which is comparable to the (^{14}C-based) estimate of *net* productivity for this region based on ^{14}C incubations (Coste *et al.*, 1977). The temporal and spatial disparities between bottle incubations and the simulation model of Klein and co-workers preclude a detailed and meaningful comparison of the two techniques for measuring the coupling between periodic nutrient pulsing and temporal- and depth-dependent productivity. The Klein-Coste model obviously must be tested with longer-term simulations, but it is possible to state at this time that, although the simulations have been short (a few days), they clearly indicate that the requisite supporting nutrient flux for "high" productivity may indeed exist.

For the most part, recycling estimates have been based both on direct measurements of excretion rates of individual zooplankton grazers together with estimates of natural population densities of these animals and on comparisons of "new" (NO_3^-) and recycled (NH_4^+) uptake rates by phytoplankton (Dugdale and Goering, 1967). Based on analyses of historical data, both Eppley and Peterson (1979) and Harrison (1980) have concluded that regeneration efficiencies increase as primary production decreases, reaching 80–90+% in oligotrophic waters. Glibert (1982), more recently, used the ^{15}N isotope dilution technique to study this problem, whereby the simultaneous rates of $^{15}NH_4^+$ uptake by phytoplankton and $^{14}NH_4^+$ excretion (dilution of ^{15}N in aqueous phase) by heterotrophs are measured. She found that, not only did excretion efficiencies reach 100% in several types of marine waters including the Sargasso Sea, but that the <10 μm size class of organisms, most likely bacteria and protozoa, was responsible for the bulk of the regeneration. These results support the growing body of recent evidence that the oceanic food web, characterized by low biomass, virtually undetectable ambient nutrients, by the appearance of steady state (Goldman *et al.*, 1979) and consisting mainly of very small phototrophs and heterotrophs, is tightly coupled in a "spinning wheel." In such a system, most of the photosynthetically-fixed

biomass is oxidized before it has a chance to sink out of the euphotic zone (Pomeroy, 1974; Sieburth *et al.*, 1978; Williams, 1981; Goldman, 1984).

The "spinning wheel" concept, at first glance, is difficult to reconcile with the notion that the oligotrophic ocean is not at steady state, that far higher new primary production occurs than previously measured, and that this increased productivity is fueled by heterogeneous inputs of new nutrients into the euphotic zone. There are, however, at least two important aspects of this problem that need to be considered. First, the bulk of nutrient regeneration data has been obtained with short-term excretion or uptake measurements on small, confined samples. Methodological and confinement problems associated with bottle incubations are as relevant to nutrient rate measurements as they are to productivity measurements (Goldman *et al.*, 1981; Glibert and McCarthy, 1984). For example, handling and confinement of large zooplankton may lead to unnatural stresses and concomitant unrepresentative rates of excretion (Bidigare, 1983). Similar problems may be associated with ^{15}N uptake and regeneration measurements. In addition, difficulties in balancing rates of ^{15}N incorporation into particulate matter with rates of ^{15}N loss from the aqueous NH_4^+ phase have hampered interpretation of NH_4^+ regeneration results based on the isotope dilution technique (Laws, 1984). One of us (JCG) has, in fact, found that certain phytoplankton species are easily damaged during the filtration and rinsing process associated with both ^{14}C and ^{15}N uptake experiments resulting in great loss of recently accumulated substrates (Goldman and Dennett, 1985). Such losses could lead to underestimates of uptake and overestimates of regeneration if labelled NH_4^+ were released during breakage. Thus there is an urgent need to evaluate the accuracy of regeneration measurements.

A second factor in trying to reconcile the controversy over new production estimates concerns the time-space scales upon which regeneration measurements are made and both the actual vertical structure of phytoplankton in the water column and the nature of new nutrient influx across the thermocline. A common characteristic of many oceanic regions is the persistence of a deep chlorophyll maximum within or just above the seasonal thermocline that is also closely associated with the nutricline. Such conditions prevail throughout most of the Pacific Ocean (Venrick *et al.*, 1973), in the Sargasso Sea (Menzel and Ryther, 1960), and in the tropical Atlantic Ocean (Herbland and Voituriez, 1979). Although there is considerable controversy as to how this relatively narrow band of chlorophyll forms at very low light levels, typically the 1% light level (Venrick *et al.*, 1973), there is good evidence that strong coupling between physical processes governing nutrient transport across the nutricline and biological processes controlling nutrient assimilation by phytoplankton can prevent the distribution of nutrients to the upper reaches of the euphotic zones (Herbland and Voituriez, 1979). Herbland and Voituriez (1979) have, in fact, shown that both integrated primary productivity and the depth of peak productivity are strongly correlated with the depth of the chlorophyll maximum.

From the above perspective the euphotic zone may be divided into two distinct regions, an upper portion void of nutrients and completely dependent on nutrient regeneration to fuel productivity—in effect, a "spinning wheel," and a lower portion dependent primarily on new nutrients from below the nutricline to regulate new production. This new production may, therefore, be processed biologically and, without ever making contact with the upper portion of the euphotic zone, sink to deeper water.

It is tempting to speculate as to the impact of this pulse-like injection of nutrients into the euphotic zone on the biology of nutrient regeneration. Eppley and Peterson (1979) and others have suggested an inverse relationship between the magnitude of net primary production and the efficiency of nutrient regeneration. That is, there appears to be, at least on a macroscopic scale, a nonlinear relationship between new production and net production rates. Dependent on the size and lifetime of the "blobs" of nutrients brought into the mixed layer, and how they compare to the patchiness and response timescales of the biota, the character of nutrient recycling (i.e. efficient vs. inefficient) may be heterogeneous. The nutrient pulses predicted by the Klein-Coste model may in fact create microcosms of eutrophic activity with concomitant inefficient nutrient recycling. These oases of activity will likely be very short-lived and limited in both vertical and horizontal extent, and thus difficult to sample directly. In fact, the pulsation of nutrient supply may stress the local food-web in such a way as to inhibit efficient regeneration of nutrients. They will likely be created at the base of the mixed layer, and with a period near that of the Coriolis period—i.e. not diurnal. Such characteristics could explain the disparity between the classical estimates of primary production/nutrient regeneration and the larger space-time integrated tracer measurements. That is, tracer measurements such as those for oxygen reflect the integrated effects of such processes, whereas the small scale "grab sampling" of ^{14}C, ^{15}N incubations may well miss the signal associated with small scale, infrequent events, and measure the "desert" conditions.

It is clear that more attention is needed regarding the detailed physics of nutrient transport into the euphotic zone. The work of Klein and Coste (1984) and others represent a marked improvement over the "classical," heavily parameterized, diffusion calculations. The nutrient flux magnitudes suggested by these more realistic estimates, combined with their pulse-like nature, point to a rather different view of primary production and nutrient regeneration in oligotrophic waters.

9. Summary

Consideration of respiration rates below the euphotic zone (Jenkins, 1982a) requires a downward carbon flux of the order 50 g C m^{-2} y^{-1} in the subtropical oligotrophic North Atlantic. When we examine the Bermuda time series hydrographic data extending over decades, the seasonal variation in oxygen due to oxidation of this newly produced carbon below the euphotic zone agrees quantitatively with this hypothesis.

The observed seasonal cycle of oxygen supersaturation within the euphotic zone (the Schulenberger-Reid effect) is consistent with the right order of magnitude of new production, but the signal is complicated by loss of oxygen both to the atmosphere and downward through the seasonal thermocline. From careful consideration of insolation effects and heat budgets it is suggested that the magnitudes of these losses are significant, and lead to estimated photosynthetic oxygen production of the order of $5M/m^2/y$. Available $^3He/^3H$ data are consistent with this rate, and a crude surface gas exchange calculation (when corrected for exsolution unloading) yields the same result. Conversion of this oxygen production term to new (carbon) primary production depends on a choice of PQ (approximately the molar ratio of oxygen produced to CO_2 fixed), but if one uses a typical range of values from 1.0 to 1.8 (Williams *et al.*, 1983), one obtains a rate of from 35 to 60 g C m^{-2} y^{-1}.

It is not realistic to use simple one-dimensional turbulent diffusion models to compute the upward flux of nutrients through the seasonal thermocline which must support this new production. The somewhat more realistic mixed layer/seasonal thermocline model used by Klein and Coste (1984) does yield fluxes of a magnitude adequate to support such high levels of new production. The nature of nutrient injection into the euphotic zone has implications regarding regeneration efficiencies.

The bulk of the evidence, based primarily on oxygen cycles within and below the euphotic zone, points to much higher levels of new production in oligotrophic waters—levels which approach the values previously thought to be characteristic of *net* productivity. This implies that either net production is actually much higher than thought, or that the efficiency of recycling within the euphotic zone is much lower. While the ^{14}C technique as a measure of net production has been challenged, it is not yet evident that errors of the order of 5 to 10 are extant in the technique. On the other hand, the possible effects of sampling, incubation and other experimental artifacts have yet to be studied completely.

The question of recycling bears further examination. The original Dugdale and Goering (1967) conclusions are based on just a few measurements, and there is a distinct possibility that the roles of photoinhibition, grazing by heterotrophs, migration, and grazing by macrozooplankton when coupled with the physics (eg. vertical turbulence, shear at the base of the mixed layer and pulsed nutrient injection) may result in vertical and temporal variations in recycling efficiency. This *in situ* variability is difficult to mimic *in vitro*, further exacerbating sampling problems. Furthermore, the variability in nutrient supply and rapid vertical motions caused by turbulence may stress the trophic structure in such a way as to impede efficient regeneration, leading to greater fluxes of carbon from the euphotic zone. If our conjecture regarding higher levels of new production in oligotrophic waters is generally true, we also need to reassess the global oceanic organic carbon budgets.

Acknowledgments. We are grateful for useful comments from W. S. Broecker, Trevor Platt and J. Steele. The computational and interpretive phase was made possible through the Center

for Analysis of Marine Systems, and the $^3He/^3H$ analytical work was supported under NSF Grant OCE81-17998 (WJJ). Support from NSF Grant OCE83-08578 (JCG) is also acknowledged. We thank TNMIK for computer graphics, and M. Harvey for patience and typing. WHOI Contribution No. 5824.

REFERENCES

Atkinson, L. P. 1973. The effect of air bubble solution on air-sea gas exchange. J. Geophys. Res., *78,* 962–968.

Barrett, J. R. 1969. Salinity changes in the western North Atlantic. Deep-Sea Res. Supp., *16,* 7–16.

Bidigare, R. R. 1983. Nitrogen excretion by marine zooplankton, *in* Nitrogen in the Marine Environment, E. J. Carpenter and D. G. Capone, eds., Academic Press, NY, 900 pp.

Broecker, H.-C., J. Peterman and W. Siems. 1978. The influence of wind on CO_2-exchange in a wind-wave tunnel, including the effects of monolayers. J. Mar. Res., *36,* 595–610.

Broecker, W. S. and T. H. Peng. 1982. Tracers in the Sea. Eldigio Press, Palisades, NY, 690 pp.

Bunker, A. F. and R. A. Goldsmith. 1979. Archived time-series of Atlantic Ocean meteorological variables and surface fluxes. Woods Hole Oceanographic Institution Tech. Rep. No. WHOI 79-3. 28 pp.

Carritt, D. E. and J. H. Carpenter. 1966. Comparison and evaluation of currently employed modifications of the Winkler Method for determining dissolved oxygen in seawater; NASCO report. J. Mar. Res., *24,* 286–318.

Coste, B., G. Jacques and H. J. Minas. 1977. Sels nutritifs et production primaire dans le Golfe du Lions et ses abords. Annal. de Instit. Oceanogr., *53,* 189–202.

Deacon, E. L. 1981. Sea-air gas transfer: the wind speed dependence. Boundary-Layer Met., *21,* 31–37.

Dugdale, R. C. and J. J. Goering. 1967. Uptake of new and regenerated forms of nitrogen in primary productivity. Limnol. Oceanogr., *12,* 196–206.

Eppley, R. W. 1980. Estimating phytoplankton growth rates in the central oligotrophic oceans, *in* Primary Productivity in the Sea, P. G. Falkowski, ed., Plenum Press, NY, 531 pp.

—— 1981. Relationships between nutrient assimilation and growth in phytoplankton with a brief review of estimates of growth rate in the ocean, *in* Physiological Bases of Phytoplankton Ecology, T. Platt, ed., Can. Bull. Fish. Aquat. Sci., *210,* 346 pp.

Eppley, R. W. and B. J. Peterson. 1979. Particulate organic matter flux and planktonic new production in the deep ocean. Nature, *282,* 677–680.

Gieskes, W. W. C., G. W. Kraay and M. A. Baars. 1979. Current ^{14}C methods for measuring primary production: gross underestimates in oceanic waters. Neth. J. Sea Res., *13,* 58–78.

Glibert, P. M. 1982. Regional studies of daily, seasonal and size fraction variability in ammonium remineralization. Mar. Biol., *70,* 209–222.

Glibert, P. M. and J. J. McCarthy. 1984. Uptake and assimilation of ammonium and nitrate by phytoplankton: indices of nutritional status for natural populations. J. Plank. Res., *6,* 677–697.

Goldman, J. C. 1984. Oceanic nutrient cycles, *in* Flows of Energy and Materials in Marine Ecosystems: Theory and Practice, M. J. R. Fasham, ed., Plenum Press, NY, 733 pp.

Goldman, J. C. and M. R. Dennett. 1985. Susceptibility of some marine phytoplankton species to cell breakage during filtration and post-filtration rinsing. J. Exp. Mar. Biol. Ecol., (in press).

Goldman, J. C., J. J. McCarthy and D. G. Peavey. 1979. Growth rate influence on the chemical composition of phytoplankton in oceanic waters. Nature, *279,* 210–215.

Goldman, J. C., C. D. Taylor and P. M. Glibert. 1981. Nonlinear time-course uptake of carbon and ammonium by marine phytoplankton. Mar. Ecol. Prog. Ser., *6,* 137–148.

Harrison, W. G. 1980. Nutrient regeneration and primary production in the sea, *in* Primary Productivity in the Sea, P. G. Falkowski, ed., Plenum Press, NY, 531 pp.

Hasse, L. and P. Liss. 1980. Gas exchange across the air-sea interface. Tellus, *32,* 470–481.

Herbland, A. and B. Voituriez. 1979. Hydrological structure analysis for estimating primary production in the tropical Atlantic Ocean. J. Mar. Res., *37,* 87–101.

Ivanoff, I. 1977. Oceanic absorption of solar energy, *in* Modelling and Prediction of the Upper Layers of the Ocean, E. B. Kraus, ed., Proc. NATO ASI, Pergamon Press, 47–71.

Jahne, B., K. O. Munnich and U. Siegenthaler. 1979. Measurements of gas exchange and momentum transfer in a circular wind-water tunnel. Tellus, *31,* 321–329.

Jenkins, W. J. 1977. Tritium helium dating in the Sargasso Sea: a measurement of oxygen utilization rates. Science, *196,* 291–292.

—— 1980. Tritium and ^{3}He in the Sargasso Sea. J. Mar. Res., *38,* 533–569.

—— 1982a. Oxygen utilization rates in the North Atlantic Subtropical Gyre and primary production in oligotrophic systems. Nature, *300,* 246–248.

—— 1982b. On the climate of a subtropical ocean gyre: decade timescale variations in water mass renewal in the Sargasso Sea. J. Mar. Res., *40* (Suppl.), 265–290.

Jenkins, W. J., W. V. Collentro and R. D. Boudreau. 1979. W.H.O.I. Helium Isotope Laboratory Data Release No. 1. W.H.O.I. Blue-Cover Report No. 79-60.

Jerlov, N. G. 1968. Optical Oceanography. Elsevier Publishing Co., Amsterdam, 194 pp.

Klein, P. and M. Coantic. 1981. A numerical study of turbulent processes in the marine upper layers. J. Phys. Oceanogr., *11,* 849–863.

Klein, P. and B. Coste. 1984. Effects of wind-stress variability on nutrient transport into the mixed layer. Deep-Sea Res., *31,* 21–37.

Laws, E. 1984. Isotope dilution models and the mystery of the vanishing ^{15}N. Limnol. Oceanogr., *29,* 379–386.

Liss, P. S. 1973. Processes of age exchange across an air-water interface. Deep-Sea Res., *20,* 221–238.

McCarthy, J. J. and E. J. Carpenter. 1983. Nitrogen cycling in near-surface waters of the open ocean, *in* Nitrogen in the Marine Environment, E. J. Carpenter and D. G. Capone, eds., Academic Press, NY, 900 pp.

Mellor, G. L. and P. A. Durbin. 1975. The structure and dynamics of the ocean surface mixed layer. J. Phys. Oceanogr., *5,* 718–728.

Menzel, D. and J. Ryther. 1960. The annual cycle of primary production in the Sargasso Sea off Bermuda. Deep-Sea Res., *6,* 351–367.

—— 1961. Annual variations in primary production of the Sargasso Sea off Bermuda. Deep-Sea Res., *7,* 282–288.

Paulson, C. A. and J. J. Simpson. 1977. Irradiance measurements in the upper ocean. J. Phys. Oceanogr., *7,* 952–956.

Peng, T.-H., W. S. Broecker, G. G. Mathieu, Y.-H. Li and A. E. Bainbridge. 1979. Radon evasion rates in the Atlantic and Pacific Oceans as determined during the GEOSECS Program. J. Geophys. Res., *84,* 2471–2486.

Peterson, B. J. 1980. Aquatic primary productivity and the ^{14}C-CO_2 method: a history of the productivity problem. Ann. Rev. System. Ecol., *11,* 359–385.

Platt, T. 1984. Primary productivity in the central North Pacific: comparisons of oxygen and carbon fluxes. Deep-Sea Res., *31,* 1311–1319.

Platt, T., M. Lewis, and R. Geider. 1984. Thermodynamics of the pelagic ecosystem: elementary closure conditions for biological production in the open ocean, *in* Flows of Energy and

Materials in Marine Ecosystems: Theory and Practice. M. J. R. Fasham, ed., Plenum Press, NY, 733 pp.

Pollard, R. G., P. B. Rhines and R. O. R. Y. Thompson. 1973. The deepening of the wind mixed layer. Geophys. Fluid Dyn., *4*, 381–404.

Pomeroy, L. R. 1974. The ocean's food web, a changing paradigm. Bioscience, *24*, 499–504.

Pransgma, G. J., T. H. Guymer, P. Kruseman, R. T. Pollard and R. A. Weller. 1983. Development of the temperature and salinity structure of the upper ocean over two months in an area 150 × 150 km. Phil. Trans. R. Soc. Lond. A, *308*, 311–325.

Riley, G. A. 1951. Oxygen, phosphate and nitrate in the Atlantic Ocean. Bull. Bingham Oceanogr. Coll., *13*, 1–126.

Sarmiento, J. L., H. W. Feely, W. S. Moore, A. E. Bainbridge and W. S. Broecker. 1976. The relationship between vertical eddy diffusion and buoyancy gradient in the deep sea. Earth Planet. Sci. Lett., *32*, 357–370.

Schulenberger, E. and J. L. Reid. 1981. The Pacific shallow oxygen minimum, deep chlorophyll maximum and primary productivity, reconsidered. Deep-Sea Res., *28*, 901–919.

Sieburth, J. McN., V. Smetacek and J. Lenz. 1978. Pelagic ecosystem structure: heterotrophic compartments of the plankton and their relationships to plankton size fractions. Limnol. Oceanogr., *23*, 1256–1263.

Smith, R. E. H., R. J. Geider and T. Platt. 1984. Microplankton productivity in the oligotrophic ocean. Nature, 311, 252–254.

Stommel, H. 1979. Determination of water mass properties of water pumped down from the Ekman layer to the geostrophic flow below. Proc. Natl. Acad. Soc. USA, *76*, 3051–3055.

Venrick, E. L., J. A. McGowan and A. W. Mantyla. 1973. Deep maxima of photosynthetic chlorophyll in the Pacific Ocean. Fish. Bull., *71*, 41–52.

Warren, B. A. 1972. The insensitivity of subtropical mode water characteristics to meteorological fluctuations. Deep-Sea Res., *19*, 1–20.

Weiss, R. F. 1970. Helium isotope effect in solution in water and seawater. Science, *168*, 247–248.

Williams, P. J. LeB. 1981. Incorporation of microheterotrophic processes into the classical paradigm of the planktonic food web. Kieler Meeresforsch. Sondeh., *5*, 1–28.

Williams, P. J. LeB., K. R. Heinemann, J. Marra and D. A. Purdie. 1983. Comparisons of ^{14}C and O_2 measurements of phytoplankton production in oligotrophic waters. Nature, *305*, 49–50.

Wise, D. L. and G. Houghton. 1966. The diffusion coefficients of ten slightly soluble gases in water 10–60°C. Chem. Eng. Soc., *21*, 999–1010.

Worthington, L. V. 1959. The 18° water in the Sargasso Sea. Deep-Sea Res., *5*, 297–305.

—— 1976. On the North Atlantic circulation. The Johns Hopkins Oceanographic Studies, No. 6, Baltimore, Johns Hopkins University Press, 110 pp.

Received: *3 July, 1984;* revised: *1 December, 1984.*